Thermo and photo-oxidation of functionalized metallocene high density polyethylene: Effect of hydrophilic groups

M.U. de la Orden[a, b, *]

mariula@ucm.es

J.M. Montes[c]

J. Martínez Urreaga[b, c]The surname is Martínez Urreaga

A. Bento[d]

M.R. Ribeiro[d]

E. Pérez[e]

M.L. Cerrada[e, **]

mlcerrada@ictp.csic.es

[a]Universidad Complutense de Madrid, Facultad de Óptica y Optometría, Dpto. Química Orgánica 1, Madrid 28037, Spain

[b]Polymers, Characterization and Applications Research Group, Spain

[c]Universidad Politécnica de Madrid, ETSI Industriales, Dpto. Ingeniería Química Industrial & Medio Ambiente, E-28006 Madrid, Spain

[d]Instituto Superior Técnico, Universidade Técnica de Lisboa, 1049-001 Lisboa, Portugal

[e]Instituto de Ciencia y Tecnología de Polímeros (ICTP-CSIC), 28006 Madrid, Spain

*Corresponding author. Universidad Complutense de Madrid, Facultad de Óptica y Optometría, Dpto. Química Orgánica 1, Madrid 28037, Spain.

**Corresponding author.Instituto de Ciencia y Tecnología de Polímeros (ICTP-CSIC), 28006 Madrid, Spain

Abstract

Incorporation of a small content of undecenoic acid is proposed as an approach to introduce polar groups within the macromolecular architecture of high density polyethylene-based materials in order to promote an easier degradation after their useful service life. The influence of these hydrophilic groups during thermo and photo-oxidation processes has been then evaluated by several complementary techniques. In addition to different degradation rates, distinct ratios of oxidized species (lactones, ketones, carboxylic acids, esters and aldehydes) are found depending on: a) the initial material (neat high density polyethylene or ethylene-*co*-undecenoic acid copolymer); b) the type of oxidation (thermo or photoinduced); and c) the absence or presence of a specific prodegradant additive. An important increase of crystallinity has been observed in the final oxidized samples, indicating that the extent of degradation is rather significant.

Keywords: Undecenoic acid; Polyethylene; Oxidation processes; Prodegradant; FTIR; Crystallinity

1 Introduction

Many of the applications (packaging, bottles, films and pipes manufacture, among others) of high density polyethylene, HDPE (the most crystalline of the commercially available PEs) are based on its chemical inertness. Although this is an advantage along the shelf life for a specific product, inertness becomes an enormous shortcoming after its useful service when proper recycling processes are not viable, since the natural decomposition process can span over many decades [1–4]. Therefore, the need for degradable polyolefins has become a hot topic in research to manage those environmental problems. An ideal solution would be the obtainment of degradable polyolefins capable of retaining functionality as

commodity plastics for the required service life but whose degradation leads to non-toxic end products in a disposal environment.

The hydrophobic nature of polyethylene (and polyolefins in general) makes it highly resistant to assimilation by microorganisms (fungi, bacteria and the like) because that hydrophobicity inhibits the growth of microflora on the polymer. It has been observed, however, for long time that the oxidation products of polyolefins can be biodegradable [5–10]. Such oxidized compounds have molar mass values that are significantly reduced and they incorporate polar oxygen-containing groups, such as acid, alcohol and ketone [11]. Consequently, a realistic approach to facilitate the final disposal would include the presence from the initial synthetic protocol of those polar groups into the hydrophobic backbone. Two main routes have been used since long time, which consists in copolymerizing ethylene with either carbon-monoxide or vinyl ketone comonomers. The former copolymers incorporate ~~into the polymer backbone~~ photo-sensitive carbonyl moieties into the polymer backbone [12] that can absorb UV light in a broad absorption band, extending beyond 340 nm [13], and can undergo primarily Norrish II reaction. This causes chain scission of the polymer to form shorter segments. Level of CO groups incorporated into the polymer chains must be limited to below 2% and some products from Dow Chemical, DuPont and Union Carbide are commercially available.

The other strategy, focused on vinyl ketone copolymers, is related to the polymerization of a vinyl monomer (such as ethylene, methyl methacrylate and styrene) containing a ketone carbonyl group at a carbon immediately adjacent to the backbone chain of the polymer [14,15]. The location of the carbonyl group is, therefore, the distinctive variation in relation to those carbon monoxide copolymers where the carbonyl group has been incorporated into the main polymer chain. The efficiency of the chain scission process changes significantly and becomes in vinyl ketone copolymers higher than that observed in the carbon-monoxide ones. The vinyl ketone copolymers have been commercialized under the trademark of Ecolyte [12].

Another approach to speed up degradation consists in adding to the polyolefin ultimate formulation suitable additives [16] (labeled as prodegradant agents) capable of promoting oxo-biodegradation processes. This is the basis for the term oxo-biodegradable polyolefins, which is used to distinguish polymers that biodegrade by a hydrolysis mechanism from those that are inert to hydrolysis but undergo oxidation [1,17]. Oxo-biodegradation then denotes a two-stage process [16] involving, in sequence, first, abiotic (photo or thermo) oxidation, and second, microbial biodegradation. Initial abiotic oxidation is an important stage as it determines the rate of the entire process. In this first period, incorporation of oxygen into the carbon backbone results in the formation of functional groups, such as carboxylic acids, esters, or aldehydes and alcohols as well. The hydrocarbon polymers change their behavior from hydrophobic to hydrophilic and chain scission can be initiated, allowing this fragmented polymer to absorb water. In the second stage, these fragments are intended to be biodegradable by microorganisms in soil or during composting.

As a new alternative, this investigation aims to trigger polyethylene oxidation (either thermo or photoreactions) by incorporation of undecenoic acid (UA) as functional comonomer, instead of the conventional carbon-monoxide or vinyl ketone ones. Functionalization methods in Ziegler–Natta polyolefin have included: the already mentioned direct copolymerization of functional comonomers [18], post-polymerization chemical modification by reactive extrusion [19], and formation of precursors that are readily converted into various functional groups by post-polymerization treatments [20]. Although the strong polar character of the carboxylic groups in the UA comonomer can lead to a very important loss of catalytic activity that might even prevent the chemical reaction, yet relatively high contents of undecenoic acid (UA) have been reported to be incorporated by direct copolymerization of ethylene using metallocene catalysts [21]. These UA groups have been selected instead of traditional comonomers owing to the recent interest of their use as compatibilizer agent in hybrid polymeric materials [22,23].

In addition to evaluation of effect of the UA presence (involved to the synthetic stage) on the thermo and photo-oxidation, the incorporation of a small amount of a prodegradant additive along the processing step will be also checked. Comparisons with the corresponding HDPE will be performed to understand the differences observed. Accordingly, synthesis of the metallocene HDPE (abbreviated as PE in the following) and the ethylene-*co*-undecenoic acid copolymer (PEU) has been carried out together with the preparation of ultimate compoundings and their characterization. Several techniques have been used to evaluate the specimens: nuclear magnetic resonance (NMR) to estimate undecenoic acid content in the copolymer; differential scanning calorimetry (DSC) and X ray diffraction (XRD) to evaluate the variations on transition temperatures and degree of crystallinity between the initial and the final thermo/photo-oxidized materials; and, finally, Fourier Transform infrared (FTIR) spectroscopy and thermogravimetric analysis for monitoring the thermo and photo-oxidation processes.

2 Experimental part

2.1 Materials

All manipulations were performed under dry nitrogen using standard Schlenk techniques. Ethylene and nitrogen (Air Liquide) were purified through absorption columns containing molecular sieves 4A and 13X. Cp_2ZrCl_2 (Aldrich), methylaluminoxane (MAO, 10 *wt.* % in toluene solution, Albemarle), and undecenoic acid (UA, Aldrich) were used as received. Toluene (Petrogal) was distilled over sodium under a dry nitrogen atmosphere, using benzophenone as indicator.

The d2w™ grade 93283 was used as prodegradant additive. It is a masterbatch based on a high density polyethylene carrier resin and was kindly supplied by Symphony Environmental, Ltd. Its melt index (at 190 °C and 2.16 kg) is 35 g/10 min and its density 0.925 g/cm^3 as indicated by its technical data sheet.

2.2 Polymerization

(Co)polymerizations were performed according to the previously reported methodology [24]. Concisely, they were carried out in a 250 cm^3 dried and nitrogen-flushed bottle for pressure reactions (Wilmad LabGlass LG-3921) magnetically stirred, using

toluene as solvent. (Co)polymerizations took place at 20 °C and 1.1 bar of ethylene. Temperature, ethylene consumption and pressure were monitored at real time using data acquisition and control software, enabling to obtain kinetic profiles. The (co)polymerizations were run until a certain amount of ethylene was consumed. (Co)polymerization mixtures were, then, quenched by the addition of acidified methanol. The HDPE homopolymer and the ethylene-*co*-undecenoic acid copolymer were collected and washed twice with methanol before drying.

Moreover, and previously to the copolymerization reaction, UA was contacted with MAO (1:3 molar equivalent) for 15 min to prevent or, at least, minimize the loss of catalyst activity and afterwards injected in the reactor. Zirconocene was also pre-contacted with MAO for 15 min. The copolymerization was started with the introduction in the reactor of the pre-activated catalyst. An ethylene-*co*-undecenoic acid copolymer (PEU) was obtained with an undecenoic acid content of 2.3 mol % as determined [25] by ^{1}H NMR.

2.3 Ultimate pristine materials

The HDPE and PEU materials synthesized in our laboratory were initially reactor powders. The neat homopolymer and copolymer as well as those that incorporate the pro-oxidant additive (in a 2 wt.% content) were processed with a corotating twin-screw microextruder (Rondol) to impose on all of them identical thermal-mechanical treatment. A screw temperature profile of 110, 145, 160, 175, and 175 °C was used from the hopper to the die, being the length-to-diameter ratio 20:1. Resulting materials were pelletized after extrusion took place. Then, thin films were obtained by compression molding at 180 °C in a hot-plate hydraulic press. Accordingly, four different initial samples were achieved, being labeled as PE_nA, PEU_nA, PE_A, and PEU_A for the homopolymer and copolymer without and with additive, respectively. In addition, T or P is appended to a given name, referring to thermo or photo-oxidized samples, respectively.

2.4 Polymer characterization

X-ray diffraction, XRD, patterns were recorded in the reflection mode by using a Bruker D8 Advance diffractometer provided with a PSD Vantec detector (from Bruker, Madison, Wisconsin). Cu Kα radiation (λ = 0.1542 nm) was used, operating at 40 kV and 40 mA. The parallel beam optics was adjusted by a parabolic Göbel mirror with horizontal grazing incidence Soller slit of 0.12° and LiF monochromator. The equipment was calibrated with different standards. A step scanning mode was employed for the detector. The diffraction scans were collected within the range of 2θ = 1–43°, with a 2θ step of 0.024° and 0.2 s per step.

Estimation of crystallinity (f_c) was carried out at room temperature from XRD profile deconvolution into the crystalline diffractions and the amorphous component using a fitting program. The error in the crystallinity determinations is estimated to be ±4 units.

Calorimetric analyses were performed in a TA Instruments Q100 calorimeter connected to a cooling system and calibrated with different standards. The sample weights ranged from 5 to 7.5 mg. A temperature interval from –40 °C to 160 °C has been studied and the used heating rate was 10 °C/min. For crystallinity determinations, a value of 290 J/g has been taken as the enthalpy of fusion of a perfectly crystalline material [26,27].

Specimens were placed in a Shel Lab oven at 70 °C for evaluating oxidation processes and their dependence on time (185 days for the HDPE-based samples and 129 days for the copolymer-based ones). Photo-degradation was carried out for 38 days within an air-conditioned chamber using an Hg lamp (G8T5, 8 W) with an emission peak at 254 nm. Samples were placed at 12 cm from the lamp and temperature was kept constant at 35 °C. All of these samples were taken out for few minutes at selected times to perform FTIR measurements along both processes.

FTIR spectra were recorded in a Nicolet iS10 spectrometer in transmission mode at a resolution of 4 cm^{-1}, with a total of 25 scans. Deconvolutions were accomplished by using the Opus 5,5™ software (Bruker Optik). Thermogravimetric analysis was carried out using a TA Instruments TGA2050 thermobalance. Samples of ~10 mg were heated at 10 °C/min from room temperature to 900 °C in dry nitrogen (30 cm^3/min).

3 Results and discussion

3.1 Structural details and phase transition location

Fig. 1 shows that crystalline structure has not been appreciably changed by the incorporation of a small amount of UA (2.3 mol %), of pro-oxidant additive (2 wt.%) or of both of them. The characteristic orthorhombic lattice is developed in all the specimens and location of the main reflections, (110) and (200) diffractions, are practically not affected, although their intensity is slightly decreased in the PEU_nA and PEU_A copolymers. This reduction is due to the fact that lateral comonomeric chains are not included within the crystalline lattice. Some studies have shown that, in general, the alkyl branches cannot enter into the polyethylene crystal lattice. Exclusively, the methyl branches are included in the crystalline cell at a substantial degree [28–30] and a small proportion of ethyl ones has been also found in crystalline environments [31,32].

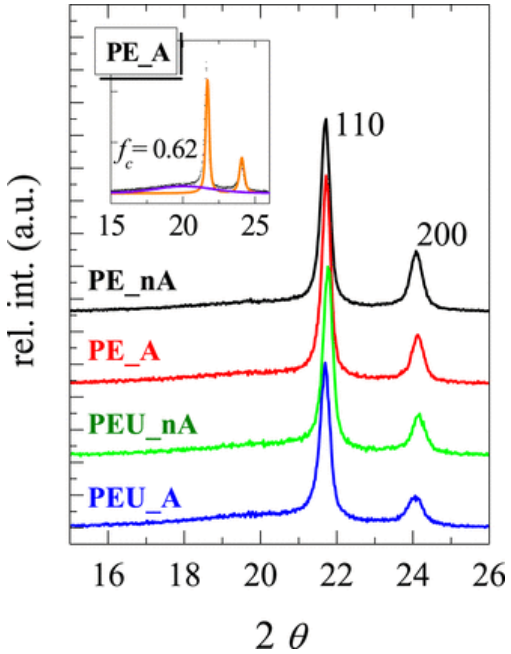

Fig. 1 X ray profiles at room temperature for the different pristine specimens evaluated. In the inset: deconvolution into the amorphous and crystalline contributions (violet and orange curves, respectively) for the PE_A sample. (Same relative scale that Fig. 3 for a better qualitative comparison). (For interpretation of the references to color in this figure legend, the reader is referred to the web version of this article.)

The commented disruption of the orthorhombic structure, because of incorporation of UA comonomer, leads, consequently, to a diminishment of crystallinity degree. Its determination has been performed as indicated in the Experimental section by deconvolution of the XRD profile into the amorphous and crystalline contributions, as shown in the inset of Fig. 1 for the PE_A sample. The values obtained are listed in Table 1. It can be seen that presence of a small amount of prodegradant additive does not affect much the crystallinity exhibited by the as-obtained initial specimens (i.e., the ones just extruded and compressed-molded samples) from the homopolymer and copolymer.

Table 1 Crystallinity degree determined from X ray experiments at room temperature for the different samples: initial ones (those attained from films after extrusion and compression molding); thermo-oxidized specimens (those achieved at the end of the thermo-oxidation process occurred within an oven at 70 °C for 185 days); and, UV oxidized samples (those obtained at the end of the UV irradiation process at 35 °C for 38 days).

Sample	Initial f_c^{xRD}	Thermo-oxidized f_c^{xRD}	Photo-oxidized f_c^{xRD}
PE_nA	0.63	0.83	0.84
PE_A	0.62	0.81	0.80
PEU_nA	0.58	0.76	0.72
PEU_A	0.56	0.76	0.72

Additional information can be acquired from calorimetric measurements. Thus, degrees of crystallinity (estimated on heating and on cooling from the melting and crystallization enthalpies, respectively) and the corresponding transition temperatures have been determined. Fig. 2 shows the DSC curves in the initial endothermic heating runs and the subsequent exothermic cooling processes for the different as-obtained pristine specimens. It is noticeable the great influence that incorporation of a small amount of UA has on the location of melting and crystallization processes (see also Table 2). Thus, a depression of the melting and crystallization temperatures (T_m and T_c, respectively) is observed in the copolymer, owing to its less compact and smaller crystallites compared with those developed in the homopolymer. In addition, the melting enthalpy is also significantly reduced in the copolymer specimens. The aforementioned introduction of UA comonomeric units hinders the chain regularity necessary for a more perfect crystallization process to take place. Consequently, crystallinity of the copolymer estimated from the melting endotherm and the cooling exotherm is lowered in the PEU copolymers, results that confirm those obtained from WAXS experiments.

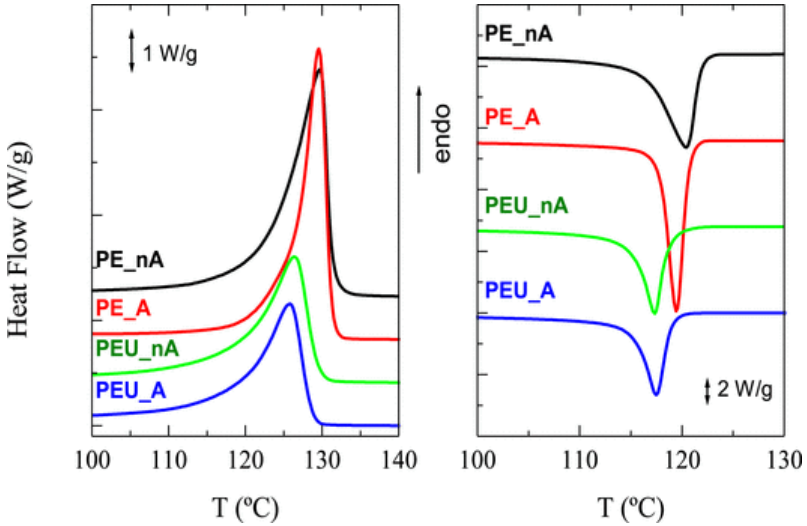

Fig. 2 Calorimetric curves for the four initial specimens evaluated: first melting runs (left plot) and subsequent cooling processes (right plot).

Table 2 Transition temperatures obtained during heating and cooling experiments (T_m and T_c, respectively) and the corresponding crystallinity degree ($f_c^{melting}$ and $f_c^{crystallization}$) determined in the pristine specimens and those thermo-oxidized (*T*).

Samples	T_m (°C)	$f_c^{melting}$	T_c (°C)	$f_c^{crystallization}$
PE_nA	129.5	0.71	120.5	0.73
PE_A	129.5	0.68	119.5	0.71
PEU_nA	126.5	0.53	117.5	0.60
PEU_A	126.0	0.58	117.5	0.59
PE_nA_T	129.5	0.82	120.0	0.74
PE_A_T	129.0	0.76	119.5	0.68
PEU_nA_T	127.0	0.64	118.0	0.62
PEU_A_T	127.5	0.71	117.5	0.65

The presence of the pro-oxidant agent leads to different effects. The melting and crystallization processes are in the additivated PE_A homopolymer much narrower than in the neat PE_nA one. This fact means that crystallite size distribution becomes more homogeneous ~~homogenous~~ in the former sample although its crystallization has been slightly postponed during cooling (see Fig. 2). The shape of the processes does not changed in the copolymer but dynamic crystallinity is enlarged in the PEU_A by the presence of the additive.

XRD and DSC measurements have been also used to learn about the final state of the samples after both oxidation processes took place: that provoked by the treatment at a given temperature and the one triggered by UV irradiation. A common characteristic, independently of being homo or copolymer and of incorporating pro-oxidant additive or not, is that oxidation process, promoted thermally or by UV irradiation, leads to a very significant increase of crystallinity, as estimated from XRD (see Fig. 3 and Table 1) and DSC experiments (Table 2). This fact could be mainly ascribed to chain scission, which induces a molar mass decrease in the macromolecules (and formation of terminal double bonds, by effect of temperature and photo exposures). Shorter chains can thus crystallize in a larger extent.

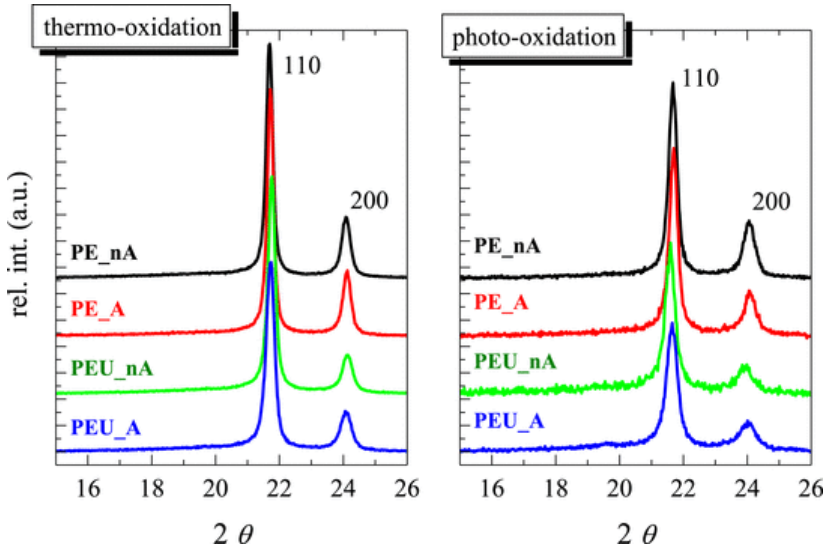

Fig. 3 X ray profiles at room temperature for the different thermo and photo-oxidized specimens (left and right, respectively).

Fig. 4 displays the crystallinity degrees estimated from XRD for the different samples. A clear increase of around 0.2 units (meaning approximately a 30% increase in crystallinity) is observed in all cases between the initial samples and the oxidized ones (with very similar values for thermo- and photo-oxidation).

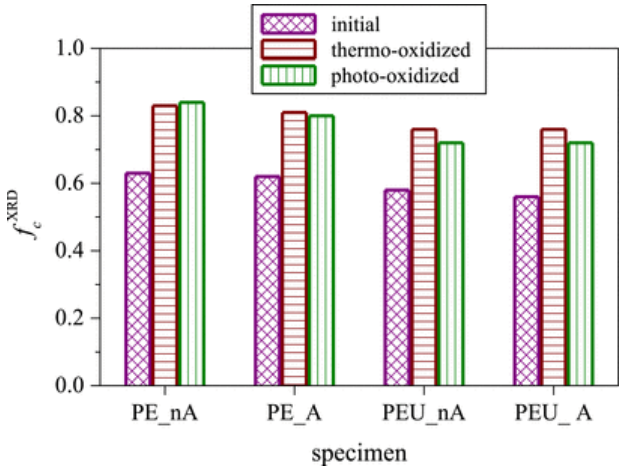

Fig. 4 Comparison of the XRD degree of crystallinity between the initial specimens and those after thermo and photo-oxidation.

In spite of the fact that the absolute XRD crystallinity achieved is similar at a given oxidized sample, it is important to remark that the widths of the (110) and (200) crystalline reflections are in those photo-oxidized specimens larger than in those thermally-degraded samples. This fact seems to indicate that photo-oxidation leads to crystallites with a broader size distribution and, consequently, to crystalline entities with more heterogeneous ~~heterogenous~~ sizes.

3.2 Time evolution of oxidation processes

Once the characteristics of the initial and ultimate thermo/photo oxidized samples are known, the analysis of how oxidation is initiated and evolves on time is an important aspect to be learnt in order to understand the mechanisms involved in the degradation processes. In a first part of this dynamic study, the oxidation products were characterized by using FTIR spectroscopy; then, the dependence on time of the spectra was used to determine the effect on the oxidation kinetics of polar groups existing in

the copolymer as well as incorporation of a pro-oxidant additive. The oxidation studies were stopped when each material became very fragile, smashed and untreatable.

Fig. 5 shows the FTIR spectra of PE (up) and PEU (down) before and after the degradation processes. The spectra were normalized using the band at 1463 cm^{-1} as internal standard, which is ascribed to the asymmetric deformation vibration of the methylene group. The spectra of the starting materials, PE_nA and PEU_nA, show the characteristic absorption bands of polyethylene [33,34] at 2915 cm^{-1} and 2847 cm^{-1}, 1463 cm^{-1} and 720 cm^{-1}. The spectrum of the copolymer also shows the presence of two additional peaks assigned to carboxyl (1710 cm^{-1}) and ester (1746 cm^{-1}) groups from the 10-undecenoic acid comonomer. These ester groups are generated in the last step of the synthesis of the copolymer, when the product is precipitated and washed with acidified methanol [27]. As mentioned in the Experimental section, the carboxylic groups of the undecenoic acid are protected with MAO during the synthesis of the copolymer to prevent the deactivation of the catalyst. The treatment of the product with acidified methanol allows the elimination of the aluminum bonded to the hydrophilic sites and, then, carboxyl and ester groups are generated.

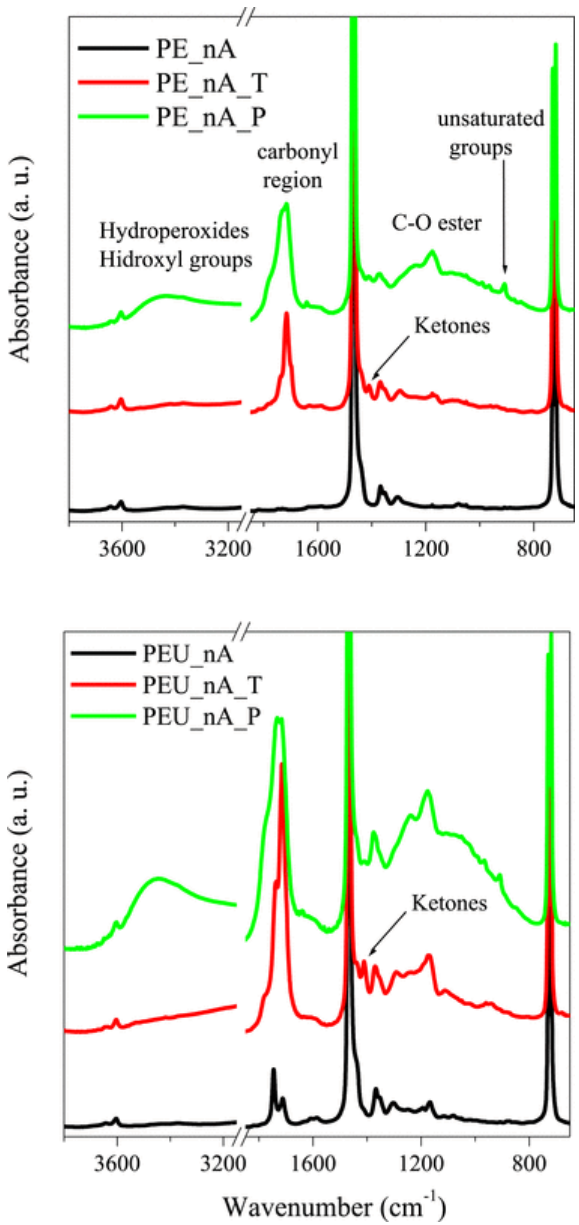

Fig. 5 FTIR spectra measured in samples before and after thermo-oxidative and photo-oxidative degradation. T and P denote thermo- and photo-oxidation, respectively.

Several new bands are observed in the spectra of the thermo-oxidized specimens. The most noticeable change corresponds to the appearance of different carbonyl group bands ranging between 1800 and 1600 cm^{-1}. This region, which is analyzed later in detail, will be used to learn the effect of incorporation of 10-undecenoic acid and pro-oxidant agent in the degradation of these materials.

There are other smaller but significant variations in other regions of the spectra. A new absorption band that appears at 1410 cm^{-1} in the spectra of the thermo-oxidized materials has been assigned by several researchers to the formation of internal ketones in the backbone chain [9,34–36]. The presence of unsaturated compounds at around 945 cm^{-1} is also detectable. The absorptions observed between 1000 and 800 cm^{-1} have been assigned to unsaturated groups [34], such as vinylidene (887 cm^{-1}),

vinyl (909 cm^{-1}) and vinylene (965 cm^{-1}). Finally, a weak but broad absorption appearing above 3000 cm^{-1} can be assigned to hydroxyl and hydroperoxide groups formed during the degradation processes [33]. All these changes seem to be in the copolymer more important than in the homopolymer.

Fig. 5 also shows the FTIR spectra of PE and PEU under photo-oxidative degradation. These spectra display several differences with respect of those obtained along the thermo-oxidation process. For example, the absorption observed at 1410 cm^{-1} in the spectra of the thermo-oxidized films, assigned to internal ketones, is scarcely noticeable in the spectra of the photo-oxidized materials. This result agrees with those reported by other authors, which conclude that one of the differences between the oxidation mechanism initiated by heat and by light is that ketone products are stable to heat but not to UV light [16,37]. The spectral zones corresponding to hydroperoxide and hydroxyl groups (above 3000 cm^{-1}) and to unsaturated compounds (between 900 and 1000 cm^{-1}) reveal other variations; the absorption due to these groups is, by far, in the samples under to photo-oxidation more important than in the thermo-oxidized ones.

A similar analysis has been carried out for the specimens that contain a pro-oxidant additive. The spectra (not shown here) reveal that the bands developed during the degradation processes of these materials are the same bands observed in the samples that do not contain the additive. None new band related to the presence of the additive was observed in the spectra of the oxidized materials.

As discussed above, the most important changes occurring during degradation appear in the carbonyl region, between 1600 and 1800 cm^{-1}. Therefore, this region has been chosen to explore in detail the effect of the 10-undecenoic acid comonomer on the degradation of polyethylene either without or with addition of a pro-oxidant additive. Fig. 6 shows the evolution on time of the absorptions bands in the carbonyl region during the thermo-oxidation at 70 °C. The degradation of each material causes the appearance of oxidation bands centered at 1700 cm^{-1}, 1714 cm^{-1}, 1734 cm^{-1} and 1780 cm^{-1}, which can be assigned to carboxylic acids, ketones, aldehydes and esters and lactones, respectively. This result, which agrees with those published by other authors [9,33–36,38–40], can be explained by the mechanisms proposed in the literature for the degradation of PE. For instance, Gugumus [41] has suggested that the main structures in the oxidation of PE are keto-hydroperoxides that lead to chain scission with simultaneous formation of carboxylic acids, aldehydes and methyl-ketone groups. Other compounds, such as olefins, esters and lactones are also formed during the degradation processes [33]. On the other hand, it is important to notice the much higher concentration of those species obtained in sample PE_A in relation to the non-additivated specimen, at similar oxidation times.

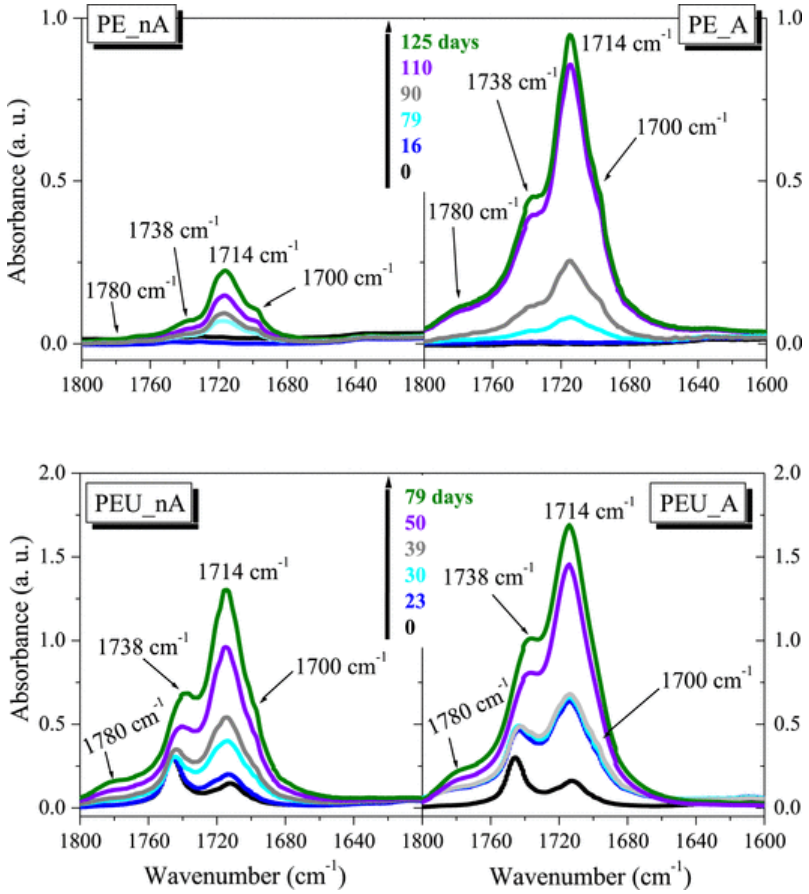

Fig. 6 Evolution of the absorption bands in the carbonyl region for the different materials during the thermo-oxidation.

The spectra of PEU, with and without pro-oxidant additive, show identical evolution that those present in PE: the initial bands centered at 1710 and at 1746 cm^{-1}, assigned to carboxyl and ester groups of comonomer, exhibit shifts towards 1714 and to 1738 cm^{-1}, respectively, which are assigned to the appearance of the carbonyl compounds produced during the thermo-oxidation. In this case, however, the differences between additivated and non-additivated samples is much smaller than in the case of PE, mainly because sample PEU_nA already shows a considerable enhancement of the degradation ability.

The time evolution of the spectra in the carbonyl region shows several differences between the specimens degraded by heat and those oxidized under UV irradiation. Fig. 7 shows the changes of the absorption bands in this region during the UV-oxidation. The bands at 1734 (aldehydes and ester) and at 1780 cm^{-1} (lactones) appear to have higher relative importance in UV-oxidation than in thermo-oxidation. Moreover, the UV-oxidized materials show an absorption band centered at 1640 cm^{-1}, assigned to unsaturated compounds, which does not appear in the spectra corresponding to thermo-oxidized samples. The above results seem to indicate that the same products, but in different relative concentration, are generated in these two oxidation processes under study.

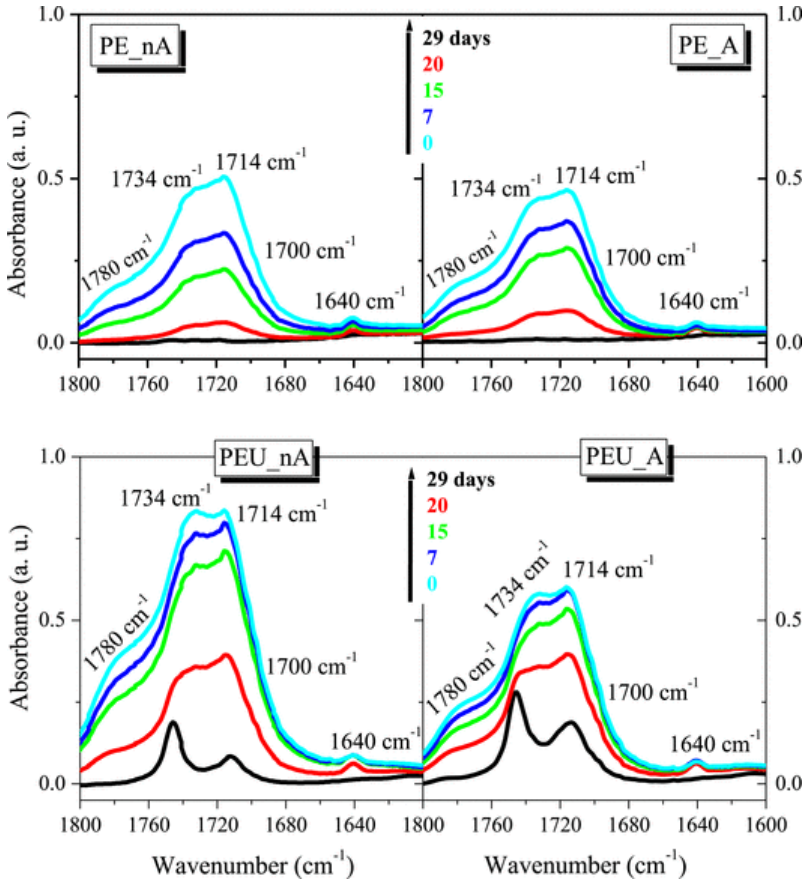

Fig. 7 Evolution observed in the carbonyl region during the photo-oxidation.

The C═O bands in the carbonyl region have been deconvoluted in order to gain information about the above-mentioned differences and the effect of 10-undecenoic acid on these degradation processes. Four absorption bands were used for the deconvolution (1700 cm^{-1}: carboxylic acids; 1714 cm^{-1}: ketones; 1734 cm^{-1}: esters and aldehydes and 1780 cm^{-1}: lactones) following the work of Lacoste and Carlsson [42], which selected these maxima from chemical derivatization studies on polyethylene subjected to gamma-, photo-, and thermally-initiated oxidation. In the copolymers, the initial absorption that corresponds to the undecenoic acid has been subtracted in order to obtain information only from the new functional groups originated during the degradation processes. Fig. 8 shows the relative contributions of the resolved bands in the different specimens evaluated in this work.

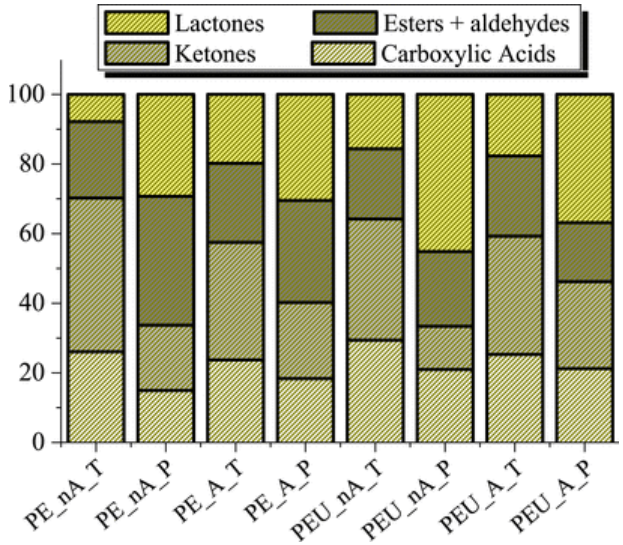

Fig. 8 Relative contributions of the four resolved bands corresponding to the carbonyl region. T and P denote thermo- and photo-oxidation, respectively.

Noticeable differences between both types of oxidation are evident from these results. The amount of ketones is in the photo-oxidized samples lower than in the thermo-oxidized ones, particularly in the materials that do not contain the pro-oxidant additive. For instance, the difference in the proportion of ketones between the thermo- and the photo-oxidized samples is as high as 25% in PE_nA, while this variation is only of 12% in PE_A. The photo-oxidized specimens also exhibit a smaller amount of carboxylic acids, and have (particularly those that do not contain the pro-oxidant agent) a ratio of lactones higher than the thermo-oxidized ones. These results can be explained by considering that the internal ketones undergo Norrish type I or type II reactions in the presence of UV radiation to produce chain end ketones, olefins, carboxylic acids, esters, aldehydes and lactones [43,44]. Thus, the occurrence of these reactions can account for the decrease in the amount of ketones and the increase in the relative proportions of the other degradation products. Moreover, it is well-known that strong photo-oxidation conditions, such as those used in this present investigation, favor the formation of lactones from carboxylic acids [45], which explain the high proportion of lactones (and the low amounts of carboxylic acids) found in the photo-oxidized materials.

Fig. 8 allows also the comparison between the final products generated in the degradation of the homopolymer and the copolymer. Although the relative amount of lactones appears to be higher in the copolymers, there are only small differences. Similarly, the relative ratio of the final products is almost independent of the presence of pro-oxidant agent.

The carbonyl index (CI) has been estimated to study the effects on the rate of the degradation of the polar groups existing in the copolymer and the incorporation of a pro-oxidant additive. The CI values are determined in this work by using the following equation:

$$\mathrm{CI} = A_{\mathrm{carbonyl}} / A_{1500-1424}$$

where A_{carbonyl} is the integrated area of the absorption bands that correspond to carbonyl groups. The selected limits for the carbonyl region were 1840 and 1640 cm^{-1} in the thermo-oxidized materials. The limits are, however, 1840 and 1660 cm^{-1} in the photo-oxidized samples in order to exclude from the values of the CI the area of the band at 1640 cm^{-1}, which corresponds to the unsaturated groups produced in the photo-oxidation. The $A_{1500-1424}$ is the integrated area of the absorption band that ascribed to the methylene groups (1500–1424 cm^{-1}), used as internal reference.

Fig. 9 shows the evolution of the CI values measured in the samples thermally maintained at 70 °C for 129 days (PEU) or 185 days (PE). The initial CI values are zero in all the materials because the initial absorption of the 10-undecenoic acid in this region was subtracted, in order to measure only the development of new functional groups during the degradation processes.

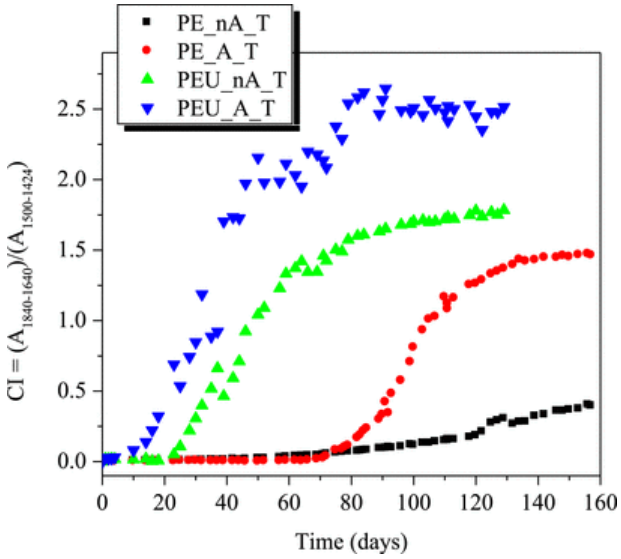

Fig. 9 Time evolution of carbonyl index (CI) values during the thermo-oxidation at 70 °C.

It is well evident that there are important differences in the oxidation kinetics between the homopolymer and the copolymer (and between the additivated and non-additivated samples). The CI of the PE homopolymer specimens increases very slightly below around 60 days, thus showing that these materials have the slowest oxidation rate. The induction period in the PEU_nA specimen lasts, however, only around 22 days. After the induction period, the thermo-oxidation in the copolymer is by far faster than in the homopolymer and the final values of the CI in the time intervals studied are significantly higher in this copolymer.

Hence, it can be commented that the undecenoic acid used as comonomer speeds up the thermo-oxidation process. There are several factors that contribute to explain this feature:

- The introduction of the comonomer causes an increase of the amount of labile hydrogen atoms in tertiary carbons. This factor was also considered by Liu et al. for explaining the degradation of copolymers of ethylene and octene [33].
- Additionally, the polar groups existing in the undecenoic acid monomer can lead to an increase in reactivity and, thereby, can promote degradation processes. It is known that the carbonyl groups present in PE favor the subsequent degradation of PE. Jacubowicz and Enebro [46] found that the addition of pre-oxidized PE causes a significant increase in the oxidation rate of PE.
- Finally, it should be taken into account that the presence of comonomer decreases the density and, therefore, increases the free volume between the polymeric chains, characteristics that makes easier the access of oxygen into the material [16]. In relation to this, comonomer incorporation reduces the crystallization capability in macromolecules because of the rupture of regularity and, then, crystallinity is significantly decreased, as aforementioned. The content of chains in an amorphous state is simultaneously raised as well as the easiness of oxygen diffusion through this disordered phase.

On the other hand, Fig. 9 also shows how the incorporation of the pro-oxidant additive affects the oxidation of PE. The evolution of the CI values during the thermo-oxidation of PE with additive exhibits two different stages, up to 70 days, i.e., in the first part of the process, the additive decreases the oxidation rate and the CI values of the PE_A sample are in fact slightly inferior than the values corresponding to the PE without additive, PE_nA specimen. At higher times, the oxidation rate increases markedly in a second step. These results can be explained if one considers that in PE_nA (and also in PEU_nA) none additives (neither antioxidant agents) have been added during processing while the commercial additive used in this work contains, together with a specific pro-oxidant compound, antioxidant agents in its composition to ensure stability of the additivated polymer during its lifetime [16]. As it could be expected, the pro-oxidant substance accelerates the thermal degradation after the period of protection of the antioxidant additive (around 70 days in these experiments). These findings are in good agreement with those reported by different researchers [9,34,35,38–40]. It has been found in all cases that the additive promotes the polyethylene degradation through free-radical chain scission reactions involving the atmospheric oxygen.

The behavior of the copolymer PEU is different. Unlike what happened in PE samples, the additive reduces the induction period in this PEU_A copolymer, which goes from 22 to 10 days. The thermo-oxidation rate is similar in the two cases PEU_nA and PEU_A, without or with pro-oxidant agent respectively, but the additive clearly increases the extent of the degradation. The results obtained in this work suggest the existence of some kind of chemical interaction between the undecenoic acid and the additive, which activates the pro-oxidant action of the additive.

The effect on the photo-oxidation of PE of the polar groups existing in the undecenoic acid has been also studied as well as that induced by the pro-oxidant additive. Fig. 10 depicts the evolution with time of the CI values in these photo-oxidized samples. It can be seen that the pro-oxidant additive does not significantly act on the photo-oxidation of PE. This result can be explained by taking into account that the additive used in this work is specifically designed to catalyze the thermo-oxidation of the polymer. There are other additives that are formulated to promote photo-oxidation processes.

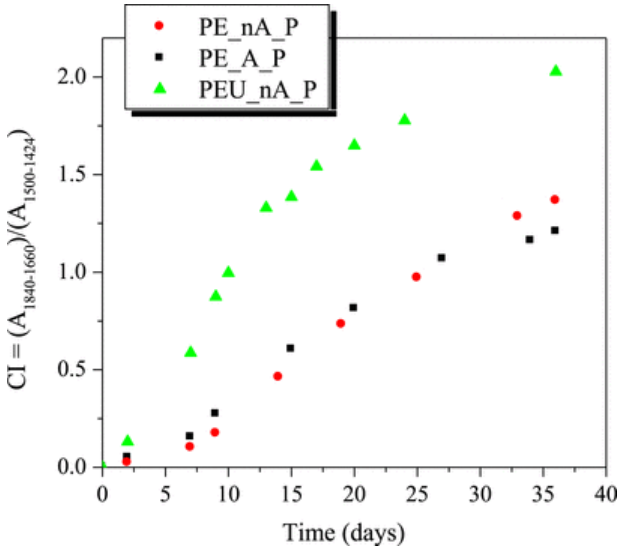

Fig. 10 Evolution on time of the carbonyl index (CI) values during the photo-oxidation at 35 °C.

Fig. 10 shows, however, that the undecenoic acid induces the photo-oxidation of the polymer, increasing both the rate and the extent of degradation, as occurred in the thermo-oxidation. This effect of the polar groups of the comonomer on the photo-oxidation can be explained by considering the same factors that have been aforementioned in the thermo-oxidation reaction.

3.3 Thermogravimetric analysis

The thermal stability of the materials before and after the oxidation processes was studied by thermogravimetric analysis under nitrogen atmosphere. Fig. 11 shows the characteristic TG curves corresponding to the four materials studied. The characteristic temperatures T_5 (temperature of 5% of weight loss, which can be considered as the onset degradation temperature) and T_{max} (temperature of maximum weight loss rate) are summarized in Table 3 for an easier comparison of the data. These results show that the thermal stability of both the homopolymer and the copolymer is significantly modified by both treatments: thermo- and photo-oxidation. Moreover, the behavior of the final materials strongly depends on how the oxidation was initiated, i.e., the TG curves corresponding to thermo-oxidized materials are clearly different to those involving the photo-oxidized ones.

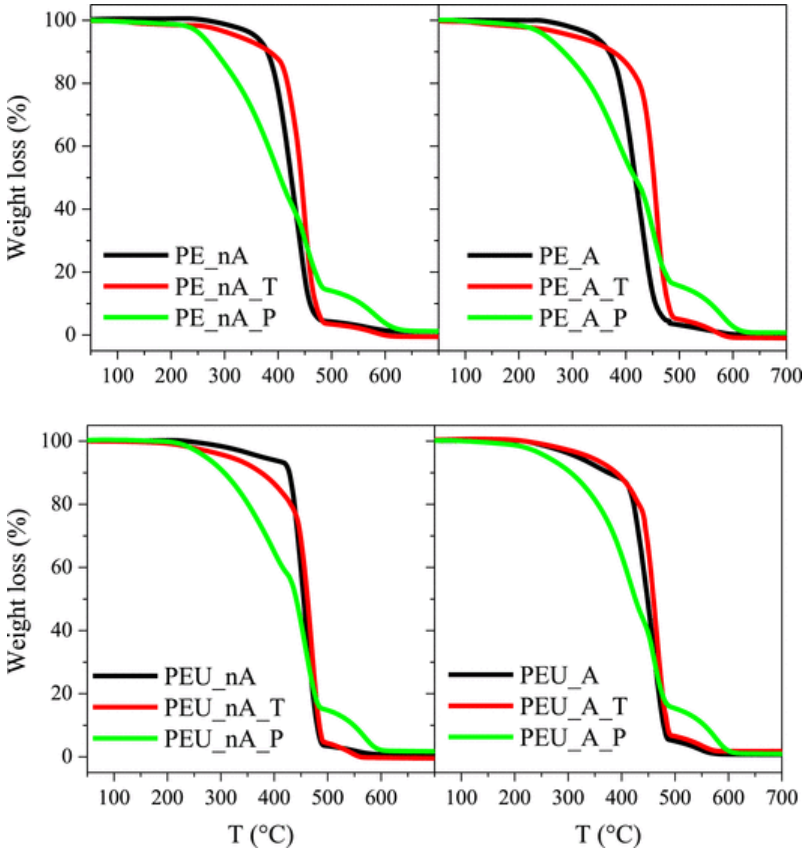

Fig. 11 TG curves measured before and after the oxidation processes. T and P denote thermo- and photo-oxidation, respectively.

Table 3 Characteristic temperatures of thermal degradation of the materials before and after thermo- and photo-oxidation.

Material		T_5 (°C)	T_{max} (°C)
PE_nA	Before degradation	357	439
	Thermo-oxidized	324	448
	Photo-oxidized	258	448
PEU_nA	Before degradation	377	454
	Thermo-oxidized	316	466
	Photo-oxidized	272	457
PE_A	Before degradation	340	436
	Thermo-oxidized	303	458
	Photo-oxidized	251	451
PEU_A	Before degradation	318	458

	Thermo-oxidized	340	464
	Photo-oxidized	261	458

Thermo-oxidation of the polymer shifts, in general, the temperature of degradation onset, T_5, to lower values. This feature can be ascribed to the formation of low-thermal stability compounds during the oxidation, as a result of the chain scission processes, which are eliminated at moderate or low temperatures. In fact, the weight loss of the thermo-oxidized materials starts at temperatures as low as 100 °C. The TG curves show, however, that, globally, the thermo-oxidized polymers have higher thermal stability than the initial ones. This result can be also observed in the values of T_{max} that are summarized in Table 3. The improvement in thermal stability can be explained as a consequence of the increase in the crosslinking density and the higher crystallinity, as already discussed, that takes place during the thermo-oxidation. Similar enlargements in crosslinking density and crystallinity during thermo-oxidation processes are well known in other polyethylenes [47].

The behavior of the photo-oxidized specimens is rather different. None increase in the overall thermal stability can be deduced from the TG curves. Only very small changes (or none changes) can be observed in the values of T_{max} while the values of T_5 display strong decreases and the weight loss at moderate or low temperatures is much more important than in the thermo-oxidized samples. Moreover, the formation of a high-thermal stability residue is clearly apparent in this case. These results have been explained as consequence of a severe process of chain scission and formation of highly crosslinked structures [48], more important than the one observed during the thermo-oxidation.

The thermal stability of the materials also depends on the presence of comonomer and pro-oxidant additive. The PEU_nA copolymer shows higher thermal stability than the homopolymer before the thermo- and photo-oxidation, as observed in the values of T_{max} and T_5. This fact has been explained by considering that the presence of the polar side groups in the copolymer promotes interactions between macromolecules and the mobility of the chains is, then, reduced. However, the values of T_5 of the oxidized copolymer (PEU_nA_T and PEU_nA_P, under thermo and photo-conditions, respectively) show reductions higher than those coming from the homopolymer (PE_nA_T and PE_nA_P). This result indicates that the comonomer promotes the degradation of the polymer during the oxidation processes, in good agreement with the above-mentioned results of the spectroscopic study.

The effect of the pro-oxidant is less clear. There are no significant changes in the values of T_{max} that can be related to the presence of the additive, but presence of the pro-oxidant additive diminishes initially the thermal stability at low temperatures of the starting materials (before imposed to the oxidation processes). The values of T_5 are in most cases lower in the materials that contain the additive, thus revealing the prodegradant activity of the additive. However, it can be found an exception in the values corresponding to the copolymer subjected to thermo-oxidation. In this case, T_5 is higher in the material that contains the additive.

4 Conclusions

Comparative studies on the thermo- and photo-oxidation of polyethylene homopolymer and a copolymer of ethylene-*co*-undecenoic acid both synthesized by using a metallocene catalyst have been performed to evaluate the effect of presence of the undecenoic acid on the oxidation processes. The incorporation of a small amount of a prodegradant additive was also checked.

The oxidation processes, promoted either thermally or by UV irradiation, lead to a very significant increase of crystallinity, as observed from calorimetric and X ray diffraction measurements, because of the chain scission reactions occurring within the macrochians, which take place preferentially in the amorphous regions.

The same products but in different relative concentrations are generated in the two oxidation processes studied. The photo-oxidation favors the formation of lactones and unsaturated compounds; while higher relative amounts of ketones and carboxylic acids are found in the thermo-oxidized specimens. The incorporation of undecenoic acid increases the amount of lactones formed in both degradation processes. The prodegradant additive used in this research accelerates the thermo-oxidation but not the photo-oxidation. The incorporation of undecenoic acid speeds up the oxidation processes, due to the increase of the amount of labile hydrogen atoms in tertiary carbons, the enhanced reactivity of the polar groups and the increase of the branching size, which increases the free volume and reduces the crystallinity and, therefore, facilitates the oxygen access. All of these results, then, indicate that incorporation of low amounts of undecenoic acid as comonomer is a suitable way to control the degradation of polyethylene.

Acknowledgements~~Acknowledgments~~

The financial support of MICINN (Project MAT2010-19883) is acknowledged as well as that received from Project CYTED 311RT0417.

References

[1]

G. Scott, Polymers and the environment, 1999, Royal Society of Chemistry; Cambridge.

[2]

J.E. Guillet, In: G. Scott, (Ed), *Degradable polymers: principles and applications,* 2nd ed., 2003, Kluwer Academic Publishers.

[3]

G. Scott and D. Gilead, In: G. Scott and D. Gilead, (Eds.), *Degradable polymers: principles and applications,* 1st ed., 1995, Chapman & Hall; London.

[4]

G. Scott and D.M. Wiles, In: G. Scott, (Ed), *Degradable polymers: principles and applications,* 2nd ed., 2003, Kluwer Academic Publishers.

[5]

J.R. Haines and M. Alexander, Microbial degradation of polyethylene glycols, *Appl Microbiol* **29**, 1975, 621–625.

[6]

A.-C. Albertsson, C. Barenstedt, S. Karlsson and T. Lindberg, Degradation product pattern and morphology changes as means to differentiate abiotically and biotically aged degradable polyethylene, *Polymer* **36**, 1995, 3075–3083.

[7]

K. Yamada-Onodera, H. Mukumoto, Y. Katsuyaya, A. Saiganji and Y. Tani, Degradation of polyethylene by a fungus, *Penicillium simplicissimum* YK, *Polym Degrad Stab* **72**, 2001, 323–327.

[8]

I. Jakubowicz, Evaluation of degradability of biodegradable polyethylene (PE), *Polym Degrad Stab* **80**, 2003, 39–43.

[9]

E. Chiellini, A. Corti and G. Swift, Biodegradation of thermally-oxidized, fragmented low-density polyethylenes, *Polym Degrad Stab* **81**, 2003, 341–351.

[10]

F. Kawai, M. Watanabe, M. Shibata, S. Yokoyama, Y. Sudate and S. Hayashi, Comparative study on biodegradability of polyethylene wax by bacteria and fungi, *Polym Degrad Stab* **86**, 2004, 105–114.

[11]

D.M. Wiles, In: R. Smith, (Ed), *Biodegradable polymers for industrial applications,* 2005, Woodhead Publishing; Cambridge.

[12]

M. Scoponi, F. Pradella and V. Carassiti, Photodegradable polyolefins. Photo-oxidation mechanisms of innovative polyolefin copolymers containing double bonds, *Coord Chem Rev* **125**, 1993, 219–230.

[13]

A.L. Andrady, J.M. Pegram and N.D. Searle, Wavelength sensitivitiy of enhanced photodegradable polethylenes, ECO, and LDPE/MX, *J Appl Polym Sci* **62**, 1996, 1457–1463.

[14]

J.E. Guillet, Photodegradable polymer compositions comprising blends of polymers with ketone containing block or graft copolymers, Pat US4176145, assigned to Guillet JE1979.

[15]

P.J. Modi and J.E. Guillet, The photochemistry of polymers containing anthrylmethyl vinyl ketone, *J Polym Sci Pol Chem* **33**, 1995, 197–201.

[16]

A. Ammala, S. Bateman, K. Dean, E. Petinakis, P. Sangwan, S. Wong, et al., An overview of degradable and biodegradable polyolefins, *Prog Polym Sci* **36**, 2011, 1015–1049.

[17]

G. Scott, *Polym Degrad Stab* **68**, 2000, 1–7.

[18]

(a) U. Giannmni, G. Bruckner, E. Pellino and A. Cassata, Polymerization of nitrogen-containing and oxygen-containing monomers by Ziegler-Natta catalysts, *J Polym Sci Part C Polym Symp* **22**, 1968, 157;

(b) C.G. Overberger and G. Khattab, *J Polym Sci Part A-I* **7**, 1969, 217;

(c) M.D. Purgett and O. Vogl, *J Polym Sci Polym Chem Ed* **27**, 1989, 2051.

[19]

M. Xanthos, Reactive extrusion. Principles and practice, 1992, Hanser Publishers; New York.

[20]

(a) T.C. Chung, Synthesis of polyalcohols via ziegler-natta polymerization, *Macromolecules* **21**, 1988, 865–869;

(b) T.C. Chung, M. Raate, E. Berluche and D.N. Schulz, Synthesis of functional hydrocarbon polymers with well-defined molecular structures, *Macromolecules* **21**, 1988, 1903–1907;

(c) S. Ramakrishnan, E. Berluche and T.C. Chung, Functional-group containing copolymers prepared by the Ziegler-Natta process, *Macromolecules* **23**, 1990, 378–382;

(d) T.C. Chung and D. Rhubright, Synthesis of functionalized polypropylene, *Macromolecules* **24**, 1991, 970–972;

(e) T.C. Chung and D. Rhubright, Functionalization of polypropylene by hydroboration, *J Polym Sci Part A Polym Chem* **31**, 1993, 2759–2763;

(f) T. Shiono, H. Kurosawa, O. Ishida and K. Soga, Synthesis of polypropylenes functionalized with secondary amino groups at the chain ends, *Macromolecules* **26**, 1993, 2085–2089;

(g) T.C. Chung, H.L. Lu and C.L. Li, Synthesis and functionalization of unsaturated polyethylene - poly(ethylene-co-1,4-hexadiene), *Macromolecules* **27**, 1994, 7533–7537.

[21]

M.L. Cerrada, R. Benavente, E. Pérez, J. Moniz-Santos, J.M. Campos and M.R. Ribeiro, Ethylene/10-undecenoic acid copolymers prepared with different metallocene catalysts, *Macromol Chem Phys* **208**, 2007, 841–850.

[22]

A. Bento, J.P. Lourenço, A. Fernandes, M.R. Ribeiro, J. Arranz-Andrés, V. Lorenzo, et al., Gas permeability properties of decorated MCM 41/polyethylene hybrids prepared by in situ polymerization, *J Membr Sci* **415–416**, 2012, 702–711.

[23]

M.L. Cerrada, E. Pérez, J.P. Lourenço, A. Bento and M.R. Ribeiro, Decorated MCM-41/polyethylene hybrids: crystalline details and viscoelastic behavior, *Polymer* **54**, 2013, 2611–2620.

[24]

J. Arranz-Andrés, V. Lorenzo, M.U. de la Orden, E. Pérez and M.L. Cerrada, Tailoring transport properties in blends based on olephinic and liquid crystalline polymers, *J Membr Sci* **377**, 2011, 141–150.

[25]

J.M. Santos, M.R. Ribeiro, M.F. Portela, S.G. Pereira, T.G. Nunes and A. Deffieux, Metallocene-catalysed copolymerisation of ethylene with 10-undecenoic acid: the effect of experimental conditions, *Macromol Chem Phys* **202**, 2001, 2195–2201.

[26]

F.A. Quinn and L. Mandelkern, Thermodynamics of crystallization in high polymers-poly-(ethylene), *J Am Chem Soc* **80**, 1958, 3178–3182.

[27]

B. Wunderlich, Macromolecular physics, 1980, Academic Press; New York.

[28]

R.G. Alamo, B.D. Viers and L. Manderkern, Phase-structure of random ethylene copolymers - a study of counit content and molecular-weight as independent variables, *Macromolecules* **26**, 1993, 5740–5747.

[29]

D.C. McFaddin, K.E. Russell, G. Wu and R.D. Heyding, Characterization of polyethylenes by X-ray-diffraction and C-13-NMR – temperature studies and the nature of the amorphous halo, *J Polym Sci Polym Phys* **31**, 1993, 175.

[30]

J. Minick, A. Moet, A. Hiltner, E. Baer and S.P. Chum, Crystallization of very low-density copolymers of ethylene with alpha-olefins, *J Appl Polym Sci* **58**, 1995, 1371.

[31]

D.L. VanderHart and E. Pérez, A C-13 NMR method for determining the partitioning of end groups and side branches between the crystalline and noncrystalline regions in polyethylene, *Macromolecules* **20**, 1986, 1902–1909.

[32]

E. Pérez, D.L. VanderHart, B. Crist and P.R. Howard, Morphological partitioning of ethyl branches in polyethylene by C-13 nuclear magneticresonance, *Macromolecules* **21**, 1987, 78–87.

[33]

Z. Liu, S. Chen and J. Zhang, Photodegradation of ethylene-octene copolymers with different octene contents, *Polym Degrad Stab* **96**, 2011, 1961–1972.

[34]

A. Benítez, J.J. Sánchez, M.L. Arnal, A.J. Müller, O. Rodríguez and G. Morales, Abiotic degradation of LDPE and LLDPE formulated with a pro-oxidant additive, *Polym Degrad Stab* **98**, 2013, 490–501.

[35]

P.K. Roy, P. Surekha, C. Rajagopal, S.N. Chatterjee and V. Choudhary, Accelerated aging of LDPE films containing cobalt complexes as prooxidants, *Polym Degrad Stab* **91**, 2006, 1791–1799.

[36]

P.K. Roy, P. Surekha, C. Rajagopal, S.N. Chatterjee and V. Choudhary, Studies on the photo-oxidative degradation of LDPE films in the presence of oxidised polyethylene, *Polym Degrad Stab* **92**, 2007, 1151–1160.

[37]

D.M. Wiles and G. Scott, Polyolefins with controlled environmental degradability, *Polym Degrad Stab* **91**, 2006, 1581–1592.

[38]

M.M. Reddy, R.K. Gupta, R.K. Gupta, S.N. Bhattacharya and R. Parthasarathy, Abiotic oxidation studies of oxo-biodegradable polyethylene, *J Polym Environ* **16**, 2008, 27–34.

[39]

E. Chiellini, A. Corti, S. D'Antone and R. Baciu, Oxo-biodegradable carbon backbone polymers – oxidative degradation of polyethylene under accelerated test conditions, *Polym Degrad Stab* **91**, 2006, 2739–2747.

[40]

X. Liu, Ch Gao, P. Sangwan, L. Yu and Z. Tong, Accelerating the degradation of polyolefins through additives and blending, *J Appl Polym Sci* **131**, 2014, 407–450.

[41]

F. Gugumus, Re-examination of the thermal oxidation reaction of polymers 3. Various reactions in polyethylene and polypropylene, *Polym Degrad Stab* **77**, 2002, 147–155.

[42]

J. Lacoste and D.J. Carlsson, Gamma-, photo-, and thermally-initiated oxidation of linear low density polyethylene: a quantitative comparison of oxidation products, *J Polym Sci Part A Polym Chem* **30** (3), 1992, 493–500.

[43]

M. Gardette, A. Perthue, J.-L. Gardette, T. Janecska, E. Fõldes, B. Pukánszky, et al., Photo- and thermal-oxidation of polyethylene: comparison of mechanisms and influence of unsaturation content, *Polym Degrad Stab* **98**, 2013, 2383–2390.

[44]

M. Bertoldo, S. Bronco, Ch Cappelli, T. Gragnoli and L. Andreotti, Combining theory and experiment to study the photooxidation of polyethylene and polypropylene, *J Phys Chem B* **107**, 2003, 11880–11888.

[45]

A. Valadez-González, J.M. Cervantes-Uc and L. Veleva, Mineral filler influence on the photo-oxidation of high density polyethylene: I. Accelerated UV chamber exposure test, *Polym Degrad Stab* **63**, 1999, 253–260.

[46]

I. Jakubowicz and J. Enebro, Effects of reprocessing of oxobiodegradable and non-degradable polyethylene on the durability of recycled materials, *Polym Degrad Stab* **97**, 2012, 316–321.

[47]

J-Il Weon, Effects of thermal ageing on mechanical and thermal behaviors of linear low density polyethylene pipe, *Polym Degrad Stab* **95**, 2010, 14–20.

[48]

S.F. Chabira, M. Sebaa, R. Huchon and B. De Jeso, The changing anisotropy character of weathered low-density polyethylene films recognized by quasi-static and ultrasonic mechanical testing, *Polym Degrad Stab* **91**, 2006, 1887–1895.

Queries and Answers

Query: Please check the country name introduced in affiliation “b” and correct if necessary.

Answer: Te affiliation b is accurate

Query: Please check the designated corresponding authors and correct if necessary.

Answer: *Corresponding author. Universidad Complutense de Madrid, Facultad de Óptica y Optometría, Dpto. Química Orgánica 1, Madrid 28037, Spain. **Corresponding author.Instituto de Ciencia y Tecnología de Polímeros (ICTP-CSIC), 28006 Madrid, Spain

Query: As Refs. [9] and [36] were identical, the latter has been removed from the reference list and subsequent references have been renumbered. Kindly check and correct if necessary.

Answer: OK. We agree

Query: Please confirm that given names and surnames have been identified correctly.

Answer: Te surname of J. Martínez Urreaga is Martínez Urreaga.